DEUTSCHES ELEKTRONEN – SYNCHROTRON

DESY 91-023
April 1991

Inclusive Production of D^0, D^+ and $D^*(2010)^+$ Mesons in B Decays and Nonresonant e^+e^- Annihilation at 10.6 GeV

ARGUS Collaboration

ISSN 0418-9833

NOTKESTRASSE 85 · D-2000 HAMBURG 52

To be sure that your preprints are promptly included in the HIGH ENERGY PHYSICS INDEX, send them to the following (if possible by air mail):

DESY
Bibliothek
Notkestrasse 85
D–2000 Hamburg 52
Germany

DESY 91-023
April 1991

ISSN 0418-9833

Inclusive Production of D^0, D^+ and $D^*(2010)^+$ Mesons in B Decays and Nonresonant e^+e^- Annihilation at 10.6 GeV

The ARGUS Collaboration

H. Albrecht, H. Ehrlichmann, T. Hamacher, G. Harder, A. Krüger, A. Nau, A. Nippe, M. Reidenbach, M. Schäfer, H. Schröder, H. D. Schulz, F. Sefkow, R. Wurth
DESY, Hamburg, Germany

R. D. Appuhn, C. Hast, G. Herrera, H. Kolanoski, A. Lange, A. Lindner, R. Mankel, M. Schieber, G. Schweda, T. Siegmund, B. Spaan, H. Thurn, A. Walther, D. Wegener
Institut für Physik[1], Universität Dortmund, Germany

M. Paulini, K. Reim, U. Volland, H. Wegener
Physikalisches Institut[2], Universität Erlangen-Nürnberg, Germany

R. Mundt, T. Oest, W. Schmidt-Parzefall
II. Institut für Experimentalphysik, Universität Hamburg, Germany

W. Funk, J. Stiewe, S. Werner
Institut für Hochenergiephysik[3], Universität Heidelberg, Germany

S. Ball, J. C. Gabriel, C. Geyer, A. Hölscher, W. Hofmann, B. Holzer, S. Khan, K. T. Knöpfle, J. Spengler
Max-Planck-Institut für Kernphysik, Heidelberg, Germany

D. I. Britton[4], C. E. K. Charlesworth[5], K. W. Edwards[6], H. Kapitza[6], P. Krieger[5], R. Kutschke[5], D. B. MacFarlane[4], R. S. Orr[5], P. M. Patel[4], J. D. Prentice[5], S. C. Seidel[5], G. Tsipolitis[4], K. Tzamariudaki[4], R. G. Van de Water[5], T.-S. Yoon[5]
Institute of Particle Physics[7], Canada

D. Ressing, S. Schael, K. R. Schubert, K. Strahl, R. Waldi, S. Weseler
Institut für Experimentelle Kernphysik[8], Universität Karlsruhe, Germany

B. Boštjančič, G. Kernel, P. Križan, E. Križnič, T. Živko
Institut J. Stefan and Oddelek za fiziko[9], Univerza v Ljubljani, Ljubljana, Yugoslavia

H. I. Cronström, L. Jönsson
Institute of Physics[10], University of Lund, Sweden

A. Babaev, V. Balagura, M. Danilov, A. Droutskoy, B. Fominykh, A. Golutvin, I. Gorelov, F. Ratnikov, V. Lubimov, A. Rostovtsev, A. Semenov, S. Semenov, V. Shevchenko, V. Soloshenko, I. Tichomirov, Yu. Zaitsev
Institute of Theoretical and Experimental Physics, Moscow, USSR

R. Childers, C. W. Darden
University of South Carolina[11], Columbia, SC, USA

[1] Supported by the German Bundesministerium für Forschung und Technologie, under contract number 054DO51P.
[2] Supported by the German Bundesministerium für Forschung und Technologie, under contract number 054ER12P.
[3] Supported by the German Bundesministerium für Forschung und Technologie, under contract number 054HD24P.
[4] McGill University, Montreal, Quebec, Canada.
[5] University of Toronto, Toronto, Ontario, Canada.
[6] Carleton University, Ottawa, Ontario, Canada.
[7] Supported by the Natural Sciences and Engineering Research Council, Canada.
[8] Supported by the German Bundesministerium für Forschung und Technologie, under contract number 054KA17P.
[9] Supported by Raziskovalna skupnost Slovenije and the Internationales Büro KfA, Jülich.
[10] Supported by the Swedish Research Council.
[11] Supported by the U.S. Department of Energy, under contract DE-AS09-80ER10690.

Abstract

Using the ARGUS detector at the e^+e^- storage ring DORIS II at DESY, we have measured the inclusive production of D^0, D^+ and $D^*(2010)^+$ mesons in B decays and in nonresonant e^+e^- annihilation around 10.6 GeV. The inclusive branching ratios for B decays to D^0, D^+ and D^{*+} mesons are found to be $(52.2 \pm 8.2 \pm 3.5)\%$, $(27.2 \pm 6.3 \pm 3.5)\%$ and $(34.8 \pm 6.0 \pm 3.5)\%$ respectively. Thus, D^0 and D^+ production account for about 70% of the charm produced in B decays, neglecting $b \to u$ contributions to the total width. The production cross sections and momentum spectra for continuum e^+e^- annihilation are also presented.

In this paper a determination of inclusive branching ratios and momentum spectra for D mesons produced in B decays is presented, where D stands for either the D^0, D^+ or $D^*(2010)^+$ meson. The dominance of $b \to c$ transitions in B decays implies that D mesons, as the lightest $c\bar{q}$ states, should be abundantly produced. Earlier measurements support this expectation [1]. The branching ratios of known exclusive hadronic final states represent approximately 9% (6%) for the neutral (charged) B decay width [2]. These modes consist mostly of a heavy $c\bar{q}$ meson plus a small number of pions. The remaining hadronic width is expected to consist of higher-multiplicity final states, resulting in a soft momentum spectrum for the charmed particle produced in these decays. Therefore, a determination of D momentum spectra provides an important constraint on possible exclusive B decays. As a byproduct of these measurements, the production cross sections and momentum spectra of D mesons in nonresonant e^+e^- annihilation at 10.6 GeV have also been determined.

The data used for this analysis have been obtained using the ARGUS detector at the e^+e^- storage ring DORIS II located at DESY. A description of the detector, its particle reconstruction and identification capabilities can be found in [3]. The data sample consists of 92.4 pb^{-1} taken on the $\Upsilon(4S)$ and 31.4 pb^{-1} taken at energies below the $\Upsilon(4S)$, with an average center-of-mass energy of 10.47 GeV. The $\Upsilon(4S)$ data sample contains 169000 ± 17200 B mesons, assuming that the $\Upsilon(4S)$ decays only into pairs of B mesons. The inclusive measurements presented are to be understood as averages over charged and neutral B mesons, in the ratio produced by $\Upsilon(4S)$ decays.

1 Selection Criteria

D mesons were reconstructed via their decays[1] $D^0 \to K^-\pi^+$, $D^+ \to K^-\pi^+\pi^+$ and $D^{*+} \to D^0\pi^+ \to K^-\pi^+\pi^+$. These are the lowest multiplicity channels consisting of charged particles only in the final state, and therefore provide the best signal-to-background ratio. This is especially of concern for D mesons from B decays, which are kinematically restricted to momenta below approximately 2.5 GeV/c.

Kaons and pions from D^0 (D^+ or D^{*+}) decays were required to have a polar angle with respect to the beamline which satisfied $|\cos\theta| < 0.85$ (0.90), thereby ensuring good momentum and dE/dx measurements in the drift chamber. In addition, the particle trajectory had to fit to the common event vertex, with the exception of the pion from the $D^{*+} \to D^0\pi^+$ decay. This particular particle is subject to sizeable deflections due to multiple scattering,

[1] References to a specific particle state should be interpreted as implying the charge-conjugate state also.

since it carries only about $1/10^{th}$ of the D^{*+} momentum due to the low Q value for the D^{*+} decay.

Particle identification was based on a likelihood ratio calculated from the available dE/dx and time-of-flight information for the allowed mass hypotheses (e, μ, π, K and p) [3]. Each particle was used as a pion or kaon if the corresponding likelihood ratio exceeded a specified value. The actual cut was chosen in order to optimize the suppression of particle misidentification while maintaining high efficiency. A small $\pi \rightarrow K$ misidentification probability is particularly important for reducing the combinatorial background. The minimum likelihood ratio values were chosen to be 10% for the D^0 and D^+ studies. A less restrictive value of 1% was used for the D^{*+} analysis, where the low Q value already results in a good signal-to-background ratio.

To reduce combinatorial background under the D^0 and D^+ signals for momentum below 2.5 GeV/c, the angle θ^*_K between the kaon flight direction in the D rest frame and the direction of the D in the laboratory frame was required to satisfy $\cos\theta^*_K < 0.8$. The distribution of $\cos\theta^*_K$ is flat for D decays but peaked at small angles for background combinations.

After these requirements, the invariant mass distributions for $K^-\pi^+$ and $K^-\pi^+\pi^+$ combinations shown in Figure 1 were obtained. For the $D^{*+} \rightarrow D^0\pi^+$ analysis, the $K^-\pi^+$ combination forming the D^0 candidate was kinematically constrained to the known D^0 mass, thereby improving the mass resolution for the D^{*+}. The plots have been broken into two intervals of the scaled momentum, $x_p = p/p_{max}$ of the D meson ($p_{max} = \sqrt{E^2_{beam} - m^2_D}$). In the low x_p region (Figure 1 a,c,e), which is kinematically allowed for B decays, there are clear D signals in the $\Upsilon(4S)$ data, but little or no evidence for production in the continuum sample. At high momentum (Figure 1 b,d,f), where only continuum production can contribute, signals appear in both data samples, reflecting the well-known hard fragmentation of charm quarks.

2 Extraction of Momentum Distributions

In order to obtain the momentum spectra, the data were subdivided into intervals of the scaled momentum x_p. The number of D mesons in each subsample was obtained by fitting the invariant mass distribution with a combination of a gaussian to describe the signal and a suitable parametrization of the background. The width of the signal in each interval was fixed to the value obtained from a linear interpolation of the observed momentum dependence of the free width. The background in the case of the D^{*+} shows no structure and has been parametrized by the function:

$$f(m) = a \cdot m \cdot (\delta m)^\alpha \cdot exp(-b \cdot \delta m)$$

where $\delta m = m - (m_{D^0} + m_{\pi^+})$. However, for the D^0 and D^+ signals the background is complicated by reflections, which demand special treatment in order to obtain a correct description of the shape.

2.1 D^0 Background

Shown in Figure 2a is an example of a D^0 fit in a typical interval of x_p. The combinatorial background under the signal has been parametrized by a third-order polynomial. Visible

in the mass interval from 1.5 to 1.7 GeV/c^2 is the well-known "satellite" peak, which is produced by selecting $K^-\pi^+$ combinations from what is actually a $D^0 \rightarrow K^-\pi^+\pi^0$ or $D^+ \rightarrow K^-\pi^+\pi^+$ decay. Ignoring this enhancement would obviously shift the background level higher, systematically reducing the fitted number of signal events. Therefore this region was excluded from the fit range, which extended from 1.3 to 2.4 GeV/c^2.

Kaons and pions with momenta above 800 MeV/c cannot be uniquely identified by the dE/dx and TOF measurements. Therefore it is rather common for the K^- and π^+ from a D^0 decay to be also accepted with the reverse assignment of particle hypotheses. The invariant mass of these doubly misidentified combinations is centered at the D^0 mass, but the width is somewhat broader than the D^0 signal itself. The probability for double misidentification depends strongly on the minimum allowed likelihood value. The clean D^0 sample from D^{*+} decays was used to determine this probability, which was found to be slightly momentum dependent with a maximum value of 30% for the cuts described above. The shape of the corresponding invariant mass distribution was parametrized using events from a Monte Carlo simulation (see below).

Slightly below the D^0 signal, a small enhancement was observed at approximately 1.76 GeV/c^2. This was identified as a reflection from the Cabibbo-suppressed decay $D^0 \rightarrow K^-K^+$, where one kaon is assigned the pion mass. The branching ratio for this decay is relatively small, but each event can produce two entries in the $K^-\pi^+$ mass distribution. The shape of the reflection was again parametrized using Monte Carlo events. Neglecting this enhancement in the background would lead to a systematic underestimate of approximately 3% in the number of signal events.

2.2 D^+ Background

An example of a fit to the $K^-\pi^+\pi^+$ invariant mass spectrum is shown in Figure 2b for a typical interval of x_p. The combinatorial background was described by the function

$$f(m) = a \cdot (\delta m)^\alpha \cdot [b \cdot exp(-c \cdot \delta m) + (1-b) \cdot exp(-d \cdot \delta m)]$$

where $\delta m = m - m_0$, m_0 a free parameter, and $0 \leq b \leq 1$. Analogous to the "satellite" peak in the D^0 invariant mass distribution, there is a visible enhancement in the $K^-\pi^+\pi^+$ spectrum between 1.2 and 1.7 GeV/c^2 produced by the decays $D^0 \rightarrow K^-\pi^+\pi^-\pi^+$ or $D^+ \rightarrow K^-\pi^+\pi^+\pi^0$, where the π^- or the π^0 respectively is neglected in calculating the invariant mass. Therefore this mass interval was excluded from the fit.

At 2.01 GeV/c^2, a D^{*+} signal from the decay $D^{*+} \rightarrow D^0\pi^+$ followed by $D^0 \rightarrow K^-\pi^+$ is expected and included in the background parametrization. Moreover, for $x_p > 0.5$, $D^0 \rightarrow K^-\pi^+$ decays produce a threshold-like rise of the background level beyond 2.0 GeV/c^2. This results from combinations of the $K^-\pi^+$ from the D^0 decay with a random π^+ from the event. The shape of this contribution was determined by Monte Carlo simulation and parametrized by an asymmetric Gaussian distribution. As the distribution of nonresonant $D^0\pi^+$ masses extends to large values, the fits were performed over the full range from 1.0 to 4.3 GeV/c^2.

3 Differential Cross Sections

The results of the fits to the $K^-\pi^+$, $K^-\pi^+\pi^+$ and $D^0\pi^+$ invariant mass distributions are listed in Tables 1-3 respectively. The systematic errors given there were obtained by varying

the widths of the signals and the reflections. For the D^0 results, the fractions of misidentified $D^0 \to K^-\pi^+$ or $D^0 \to K^-K^+$ decays were also varied. The acceptances given in the tables were determined by Monte Carlo simulation. For continuum $e^+e^- \to c\bar{c}$ events the Lund event generator [4] was used, including the effects of initial-state radiation. A modified version of the Lund program was also used to simulate B meson decays in $\Upsilon(4S) \to B\bar{B}$ events. The generated events were passed through a detailed simulation of the detector and then reconstructed with the same program as the data. The acceptances include the trigger efficiency, the selection criteria for multihadron events and losses due to the various cuts noted above.

Since the treatment of radiative corrections in continuum events is not without ambiguity, we discuss the procedure in the following. The total hadronic cross section is (to order α^3):

$$\sigma(s) = \sigma_0(s)\Big[1 + \delta + \int_{kmin}^{kmax} D\left(\frac{k}{E}\right)\frac{\sigma_0(\hat{s})}{\sigma_0(s)}\,dk\Big]$$

where σ_0 denotes the first-order cross section, δ corrections due to vacuum polarization and where $D(\frac{k}{E})\sigma_0(\hat{s})$ is the cross section for emission of a radiative photon of energy k, resulting in a reduced mass $\hat{s} = s(1 - k/E)$ for the hadronic system (E being the beam energy). The event acceptance of a detector is a function of k, it is large for $k \approx 0$, where the radiative cross section has a maximum. The acceptance decreases steeply for $k \to E$, where the radiative cross section rises again due to the small $\hat{s}$. In the acceptance correction of inclusive spectra, one can either correct back to the first-order cross section $\sigma_0(s)$ (which, strictly speaking, involves a deconvolution of inclusive spectra), or correct back to $\sigma(s)$. The latter is generally somewhat awkward, since in the limit of large k and hence of small $\hat{s}$, events usually do not pass the selection critera, and the acceptance correction relies heavily on the assumptions for $\sigma_0(\hat{s})$. Fortunately, for charm production $\hat{s} > 4m_D^2$ and hence (for $\sqrt{s} \approx 10$ GeV) $k/\sqrt{s} < 0.4$, so that this problem does not arise, and one has a reasonably flat acceptance for all allowed values of k. Therefore, we quote our results on inclusive charm yields in terms of $\sigma(s)$.

After correcting the extracted continuum and $\Upsilon(4S)$ results for acceptance and scaling by a factor of 2.89 to account for the differences in the integrated luminosities and center-of-mass energies of the continuum and $\Upsilon(4S)$ data samples, the momentum spectra shown in Figure 3 were obtained. The abundant production of D mesons in B decays is evident in the $\Upsilon(4S)$ data at low momenta, while at higher momenta, where continuum production alone contributes, the spectra are in good agreement.

3.1 Continuum Production

The production cross sections for D mesons in nonresonant e^+e^- annihilation were obtained by simply integrating the acceptance-corrected momentum spectra in the continuum data sample (Figure 4). To improve the statistical precision at high x_p, the continuum and $\Upsilon(4S)$ data samples have been combined in the region $x_p > 0.6$ for the D^0 and D^+ studies, and $x_p > 0.55$ for the D^{*+}, before extracting the momentum spectra as in Section 2 above. The extrapolation of the D^{*+} spectrum to the full momentum range was made using the Lund fragmentation function [5], since the efficiency for reconstructing D^{*+} decays vanishes at low momentum:

$$f(z) = a \cdot \frac{(1-z)^\alpha}{z} \cdot exp\left(-\frac{\beta m_T^2}{z}\right)$$

where $m_T = \sqrt{m^2 + (p_T/c)^2}$ is the transverse mass of the meson and $z = (E+pc)_{hadron}/(E+pc)_{quark}$. Although the results are shown in the figure as a function of x_p, the fragmentation fit was performed using the scaling variable $x_E = E_D/E_{beam}$ as an approximation for z. The cross sections obtained, without radiative corrections, were:

$$\begin{aligned}
\sigma_{D^0} &= (1.18 \pm 0.15 \pm 0.08)\ nb \\
\sigma_{D^+} &= (0.65 \pm 0.09 \pm 0.09)\ nb \\
\sigma_{D^{*+}} &= (0.69 \pm 0.08 \pm 0.07)\ nb
\end{aligned}$$

using values for the relevant branching ratios as given by the particle data group [7], i.e. $BR(D^0 \to K^-\pi^+) = 0.0371 \pm 0.0025$, $BR(D^+ \to K^-\pi^+\pi^+) = 0.077 \pm 0.010$ and $BR(D^{*+} \to D^0\pi^+) = 0.55 \pm 0.04$. The first error is the combined statistical and systematic uncertainty of our measurement, the second error comes from the D branching ratios. The sum of the D^0 and D^+ cross sections accounts for more than 70% of the total charm cross section at 10.55 GeV as derived by the CLEO collaboration from their measured hadronic cross section [6].

The acceptance-corrected spectra do not directly reflect the underlying fragmentation process, since the effects of initial-state radiation, which tend to soften the observed spectra, have not been removed. More importantly, most D^0 and D^+ mesons are produced by decays of D^* mesons or higher-mass D resonances [8]. Even D^{*+} production is not a particularly good measure of the fundamental fragmentation processes, since a sizeable fraction here too originate from higher-mass D or D_S resonances [9], resulting in a softer momentum spectrum. Therefore, the cross sections shown in Figure 4 and given in Tables 1-3 are presented without radiative corrections. For comparison, corresponding continuum measurements from CLEO [10] are also shown. In general, the agreement between the results is good, with the possible exception of low momentum D^0 mesons.

3.2 Inclusive B Decays

Most of the continuum cross section for D production is concentrated at high momentum. Moreover, the number of continuum events is statistically limited in comparison with the $\Upsilon(4S)$ data sample. Therefore, the precision of the measurement at low x_p, where the continuum contribution must be subtracted from the $\Upsilon(4S)$ distribution, has been improved by fitting the observed continuum spectrum with the Lund fragmentation function. The results of the fits, shown as the solid curves in Figure 3, describe the data well. The corresponding numbers of D mesons per x_p bin are given in Tables 1-3. The improvement in the precision of the continuum subtraction is clearly evident.

After subtracting the fitted continuum values from the measured $\Upsilon(4S)$ spectrum, and correcting for the difference in acceptances between continuum and $\Upsilon(4S)$ events, the momentum spectra for $B \to D^0X$, D^+X and $D^{*+}X$ shown in Figure 5 and listed in Table 4 are obtained. The extrapolation of the D^{*+} spectrum to zero momentum was made using the observed shape of the D^0 spectrum. All three spectra appear to be rather soft, indicating a sizeable fraction of multibody B decays. The products of branching ratios obtained by integrating these results are:

$$\begin{aligned}
BR(B \to D^0X) \cdot BR(D^0 \to K^-\pi^+) &= 0.0194 \pm 0.0015 \pm 0.0025 \\
BR(B \to D^+X) \cdot BR(D^+ \to K^-\pi^+\pi^+) &= 0.0209 \pm 0.0027 \pm 0.0040 \\
BR(B \to D^{*+}X) \cdot BR(D^{*+} \to D^0\pi^+) \cdot BR(D^0 \to K^-\pi^+) &= 0.0071 \pm 0.0006 \pm 0.0012
\end{aligned}$$

where the first error is statistical and the second systematic. Both the measured products of branching ratios, and the actual shape of the observed momentum spectra, are in excellent agreement with results reported by CLEO [1].

Again using average branching ratios given by the particle data group [7], the following inclusive results are obtained:

$$\begin{aligned} BR(B \to D^0 X) &= 0.522 \pm 0.082 \pm 0.035 \\ BR(B \to D^+ X) &= 0.272 \pm 0.063 \pm 0.035 \\ BR(B \to D^{*+} X) &= 0.348 \pm 0.060 \pm 0.035 \end{aligned}$$

where the first error combines the statistical and systematic uncertainty of our measurement while the second error reflects the error on the D branching ratios. If one neglects $b \to u$ transitions and assumes a probability of 15% for the creation of a $c\bar{s}$ pair from the W, the sum of the $B \to D^0 X$ and $B \to D^+ X$ branching ratios accounts for 70% of the charm produced in B decays.

It is informative to compare the extracted momentum spectra with a recent theoretical calculation based on the form-factor expansion for the $B \to D$ or D^* matrix elements [11]. This model assumes that the $b \to c$ transition is dominated by the formation of D and D^* mesons from the charm and spectator quark. The influence of the final state X on the momentum spectra of the D or D^* is included via transverse and longitudinal spectral functions. The hadronic part of these functions consists of a one-particle contribution plus a hadronic continuum. For the D^0 and D^+ spectra, feeddown from D^* decays was included, assuming a primary D^*:D=3:1 production ratio. Predictions for the D momentum spectra are shown in Figures 5a,b,c as the solid lines. Except for some deviation in the D^0 case, there is satisfactory agreement with our data.

3.3 Conclusions

In summary, we have measured the branching ratios for inclusive production of D^0, D^+ and D^{*+} mesons in B decays. The momentum spectra are soft and do not show a strong contribution from two-body B decays. The sum of the inclusive D^0 and D^+ branching ratios accounts for about 70% of the charm produced in B decays. Furthermore, production cross sections and momentum spectra for D meson created in nonresonant e^+e^- annihilation have been presented.

Acknowledgements

It is a pleasure to thank U.Djuanda, E.Konrad, E.Michel, and W.Reinsch for their competent technical help in running the experiment and processing the data. We thank Dr.H.Nesemann, B.Sarau, and the DORIS group for the excellent operation of the storage ring. The visiting groups wish to thank the DESY directorate for the support and kind hospitality extended to them.

Tables

	$\Upsilon(4S)$		Continuum			
x_p	η	$N[D^0]$	η	$N[D^0]^{scaled}$	$N[D^0]^{fitted}$	$s \cdot BR \cdot d\sigma/dx_p$
0.0 – 0.1	0.56	177 ± 34 ± 18	0.52	0 ± 46 ± 6	9 ± 4	0.0 ± 1.09 ± 0.0
0.1 – 0.2	0.49	382 ± 61 ± 34	0.42	49 ± 87 ± 9	32 ± 12	1.45 ± 2.51 ± 0.24
0.2 – 0.3	0.48	573 ± 55 ± 30	0.48	46 ± 72 ± 6	97 ± 27	1.27 ± 2.04 ± 0.21
0.3 – 0.4	0.47	639 ± 44 ± 31	0.42	132 ± 55 ± 6	178 ± 32	3.88 ± 1.59 ± 0.35
0.4 – 0.5	0.47	375 ± 33 ± 13	0.47	332 ± 49 ± 12	325 ± 35	9.80 ± 1.44 ± 0.76
0.5 – 0.6	0.53	449 ± 36 ± 15	0.47	410 ± 58 ± 12	411 ± 29	10.70 ± 1.51 ± 0.78
0.6 – 0.7		395 ± 31 ± 14	0.47	408 ± 55 ± 15	402 ± 24	10.35 ± 0.70 ± 0.77
0.7 – 0.8		291 ± 25 ± 12	0.49	292 ± 43 ± 15	305 ± 18	7.28 ± 0.55 ± 0.60
0.8 – 0.9		154 ± 18 ± 7	0.52	156 ± 29 ± 9	149 ± 14	3.62 ± 0.35 ± 0.36
0.9 – 1.0		27 ± 8 ± 2	0.52	3 ± 12 ± 0	22 ± 5	0.51 ± 0.16 ± 0.06

Table 1: Fit results and acceptance (η) for the D^0 signal in $K^-\pi^+$ invariant mass distributions and the D^0 momentum spectrum in nonresonant e^+e^- annihilation events at 10.6 GeV in units of nb · GeV^2, after luminosity scaling. The 'fitted' numbers are obtained by a fit of the Lund fragmentation function to the data (see text).

	$\Upsilon(4S)$		Continuum			
x_p	η	$N[D^+]$	η	$N[D^+]^{scaled}$	$N[D^+]^{fitted}$	$s \cdot BR \cdot d\sigma/dx_p$
0.0 – 0.1	0.43	63 ± 43 ± 32	0.37	0 ± 15 ± 0	12 ± 5	0.0 ± 0.46 ± 0.0
0.1 – 0.2	0.41	289 ± 90 ± 35	0.37	0 ± 49 ± 0	46 ± 16	0.0 ± 1.59 ± 0.0
0.2 – 0.3	0.38	504 ± 88 ± 63	0.38	136 ± 107 ± 9	103 ± 29	4.41 ± 3.45 ± 0.45
0.3 – 0.4	0.41	688 ± 73 ± 35	0.38	191 ± 101 ± 30	179 ± 36	6.08 ± 3.25 ± 1.00
0.4 – 0.5	0.41	472 ± 58 ± 19	0.38	376 ± 90 ± 9	256 ± 36	11.87 ± 2.84 ± 0.93
0.5 – 0.6	0.48	393 ± 50 ± 10	0.43	402 ± 87 ± 23	342 ± 34	11.22 ± 2.41 ± 1.00
0.6 – 0.7		345 ± 40 ± 13	0.45	318 ± 64 ± 9	351 ± 26	9.20 ± 0.95 ± 0.71
0.7 – 0.8		302 ± 29 ± 11	0.46	176 ± 38 ± 3	285 ± 18	6.94 ± 0.64 ± 0.59
0.8 – 0.9		191 ± 20 ± 5	0.49	185 ± 35 ± 6	175 ± 15	4.74 ± 0.44 ± 0.42
0.9 – 1.0		54 ± 11 ± 3	0.51	26 ± 15 ± 3	45 ± 9	1.02 ± 0.21 ± 0.17

Table 2: Fit results and acceptance (η) for the D^+ signal in $K^-\pi^+\pi^+$ invariant mass distributions and the D^+ momentum spectrum in nonresonant e^+e^- annihilation events at 10.6 GeV in units of nb · GeV^2, after luminosity scaling. The 'fitted' numbers are obtained by a fit of the Lund fragmentation function to the data (see text).

x_p	$\Upsilon(4S)$		Continuum			
	η	N$[D^{*+}]$	η	N$[D^{*+}]^{scaled}$	N$[D^{*+}]^{fitted}$	$s \cdot BR \cdot d\sigma/dx_p$
$0.11 - 0.25$	0.22	$97 \pm 14 \pm 4$	0.19	$9 \pm 12 \pm 0$	5 ± 2	$0.33 \pm 0.57 \pm 0.05$
$0.25 - 0.35$	0.39	$166 \pm 16 \pm 9$	0.39	$6 \pm 15 \pm 6$	20 ± 6	$0.19 \pm 0.46 \pm 0.15$
$0.35 - 0.45$	0.48	$164 \pm 15 \pm 7$	0.47	$46 \pm 15 \pm 3$	51 ± 10	$1.21 \pm 0.39 \pm 0.12$
$0.45 - 0.55$	0.48	$123 \pm 13 \pm 5$	0.49	$119 \pm 23 \pm 6$	92 ± 10	$2.93 \pm 0.55 \pm 0.25$
$0.55 - 0.65$		$134 \pm 12 \pm 3$	0.48	$93 \pm 17 \pm 3$	124 ± 9	$3.08 \pm 0.27 \pm 0.23$
$0.65 - 0.75$		$137 \pm 12 \pm 4$	0.49	$150 \pm 23 \pm 6$	141 ± 9	$3.49 \pm 0.24 \pm 0.26$
$0.75 - 0.85$		$116 \pm 11 \pm 5$	0.47	$98 \pm 17 \pm 3$	113 ± 8	$2.85 \pm 0.24 \pm 0.23$
$0.85 - 1.0$		$59 \pm 8 \pm 3$	0.47	$75 \pm 15 \pm 0$	62 ± 9	$1.08 \pm 0.12 \pm 0.08$

Table 3: Fit results and acceptance (η) for the D^{*+} signal in $D^0\pi^+$ invariant mass distributions and the D^{*+} momentum spectrum in nonresonant e^+e^- annihilation events at 10.6 GeV in units of nb $\cdot$ GeV^2, after luminosity scaling. The 'fitted' numbers are obtained by a fit of the Lund fragmentation function to the data (see text).

p $[GeV/c]$	$\frac{BR_{D^0}}{N_B} \cdot \frac{dN_{D^0}}{dp}$ $[10^{-3} \cdot c/GeV]$	$\frac{BR_{D^+}}{N_B} \cdot \frac{dN_{D^+}}{dp}$ $[10^{-3} \cdot c/GeV]$	p $[GeV/c]$	$\frac{BR_{D^{*}\cdot}BR_{D^0}}{N_B} \cdot \frac{dN_{D^{*}+}}{dp}$ $[10^{-3} \cdot c/GeV]$
$0.0 - 0.5$	$3.6 \pm 0.8 \pm 0.6$	$1.4 \pm 1.2 \pm 0.8$	$0.0 - 0.5$	$1.23 \pm 0.30 \pm 0.19$
$0.5 - 1.0$	$8.5 \pm 1.5 \pm 1.3$	$7.1 \pm 2.7 \pm 1.2$	$0.5 - 1.2$	$3.57 \pm 0.52 \pm 0.59$
$1.0 - 1.5$	$12.1 \pm 1.5 \pm 1.6$	$12.7 \pm 2.9 \pm 2.2$	$1.2 - 1.7$	$4.52 \pm 0.52 \pm 0.73$
$1.5 - 2.0$	$11.7 \pm 1.4 \pm 1.5$	$15.0 \pm 2.4 \pm 1.9$	$1.7 - 2.2$	$2.85 \pm 0.45 \pm 0.37$
$2.0 - 2.5$	$2.3 \pm 1.1 \pm 0.3$	$4.9 \pm 2.0 \pm 0.7$	$2.2 - 2.7$	$0.79 \pm 0.43 \pm 0.10$
$2.5 - 3.0$	$1.0 \pm 1.0 \pm 0.1$	$1.2 \pm 1.5 \pm 0.2$	$2.7 - 3.2$	$0.11 \pm 0.18 \pm 0.01$
$3.0 - 3.5$	$-0.1 \pm 0.5 \pm 0.0$	$0.0 \pm 0.6 \pm 0.0$	$3.2 - 3.7$	$-0.04 \pm 0.18 \pm 0.0$

Table 4: Momentum spectra of D^0, D^+ and D^{*+} mesons from inclusive B decays

Figure Captions

Figure 1 Distribution of invariant masses for D^0 (a,b) D^+ (c,d) and D^{*+} (e,f) mesons in the $\Upsilon(4S)$ (crosses) and continuum (hatched) data samples.

Figure 2 Typical mass spectra for (a) D^0 and (b) D^+ mesons illustrating the fitting procedure.

Figure 3 Acceptance corrected momentum spectra of (a) D^0, (b) D^+ and (c) D^{*+} mesons in the $\Upsilon(4S)$ (full circles) and continuum (open circles) data samples. The solid curve is a fit of the Lund fragmentation function to the continuum spectrum (see text).

Figure 4 Differential cross sections for (a) D^0, (b) D^+ and (c) D^{*+} mesons in nonresonant e^+e^- annihilation events from this analysis (full circles) and from CLEO [10] (open circles). The curves show the result of fitting the Lund fragmentation function to our data.

Figure 5 Momentum spectra in the $\Upsilon(4S)$ rest frame for (a) D^0, (b) D^+ and (c) D^{*+} mesons from inclusive B decays. The curves are results of a calculation of Wirbel and Wu [11], normalized to the data. For the D^0 and D^+ spectra, a feeddown from D^* decays assuming a primary D^*:D=3:1 production ratio was included.

References

[1] D. Bortoletto *et al.* (CLEO), Phys. Rev. **D35** (1987) 19.

[2] H. Albrecht *et al.* (ARGUS), Z. Phys. **C48** (1990) 543.

[3] H. Albrecht *et al.* (ARGUS), Nucl. Instr. Meth. **A275** (1989) 1.

[4] T. Sjöstrand, Com. Phys. Comm. **27** (1982) 243;
T. Sjöstrand, Com. Phys. Comm. **28** (1983) 229;
T. Sjöstrand, Com. Phys. Comm. **39** (1986) 347.

[5] B. Andersson *et al.*, Z. Phys. **C20** (1983) 317.

[6] T. Bowcock *et al.* (CLEO), Phys. Rev. **D38** (1988) 2679.

[7] Particle Data Group, Phys. Lett. **B239** (1990).

[8] H. Albrecht *et al.* (ARGUS), Phys. Lett. **B221** (1989) 422, Phys. Lett. **B231** (1989) 208.

[9] H. Albrecht *et al.* (ARGUS), Phys. Rev. Lett. **56** (1986) 549, Phys. Lett. **B230** (1989) 162

[10] D. Bortoletto *et al.* (CLEO), Phys. Rev. **D37** (1988) 1719.

[11] M. Wirbel and Y.-L. Wu, Phys. Lett. **B228** (1989) 430.

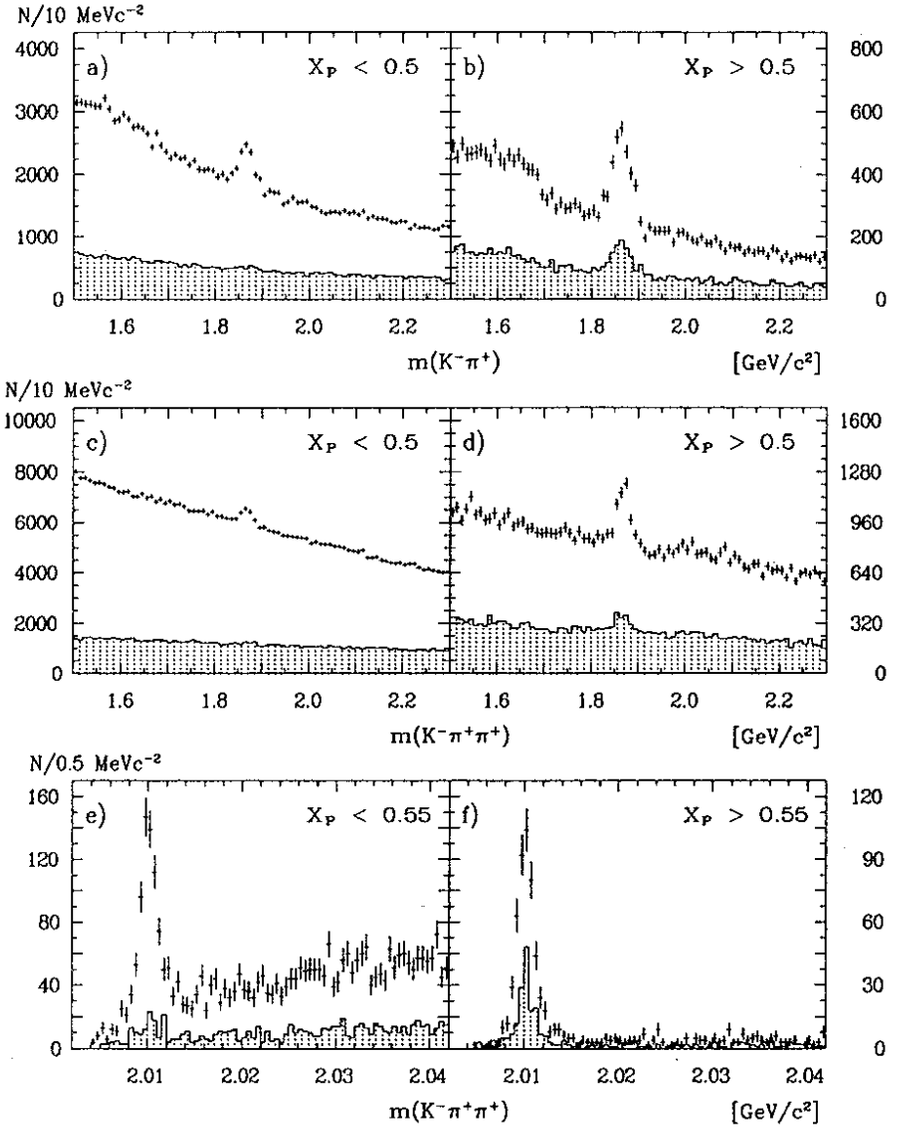

Figure 1

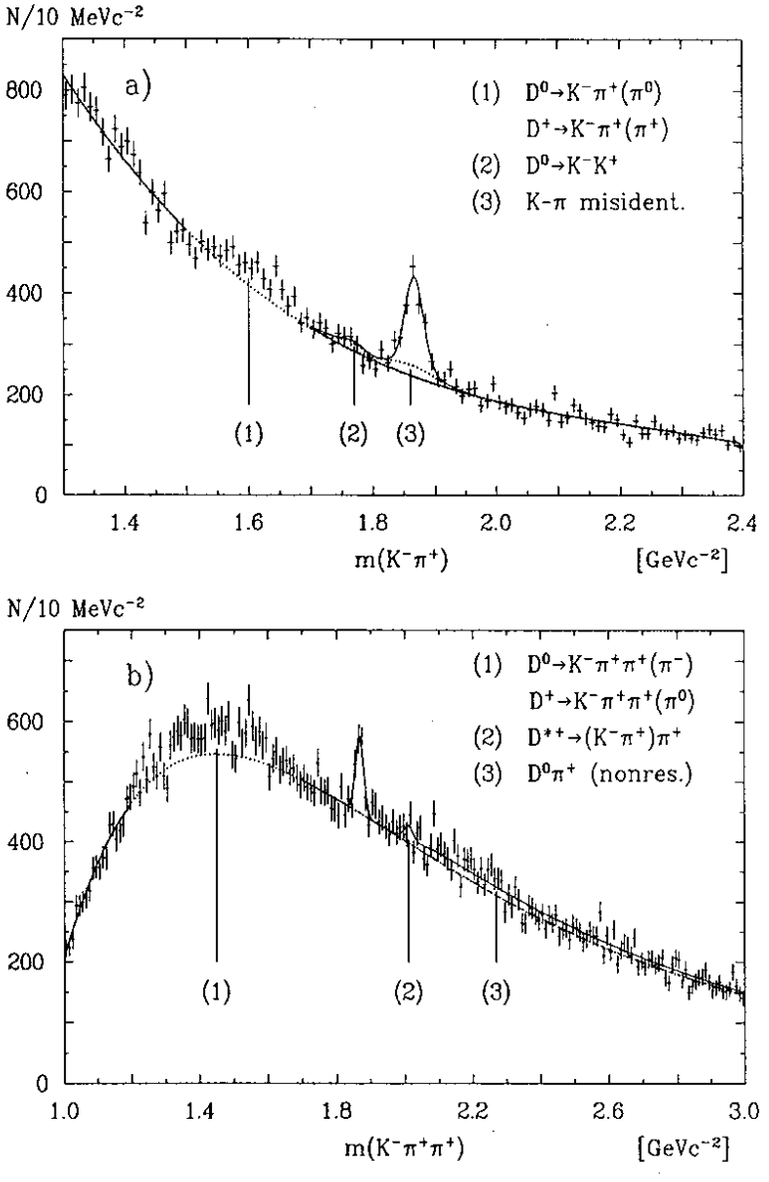

Figure 2

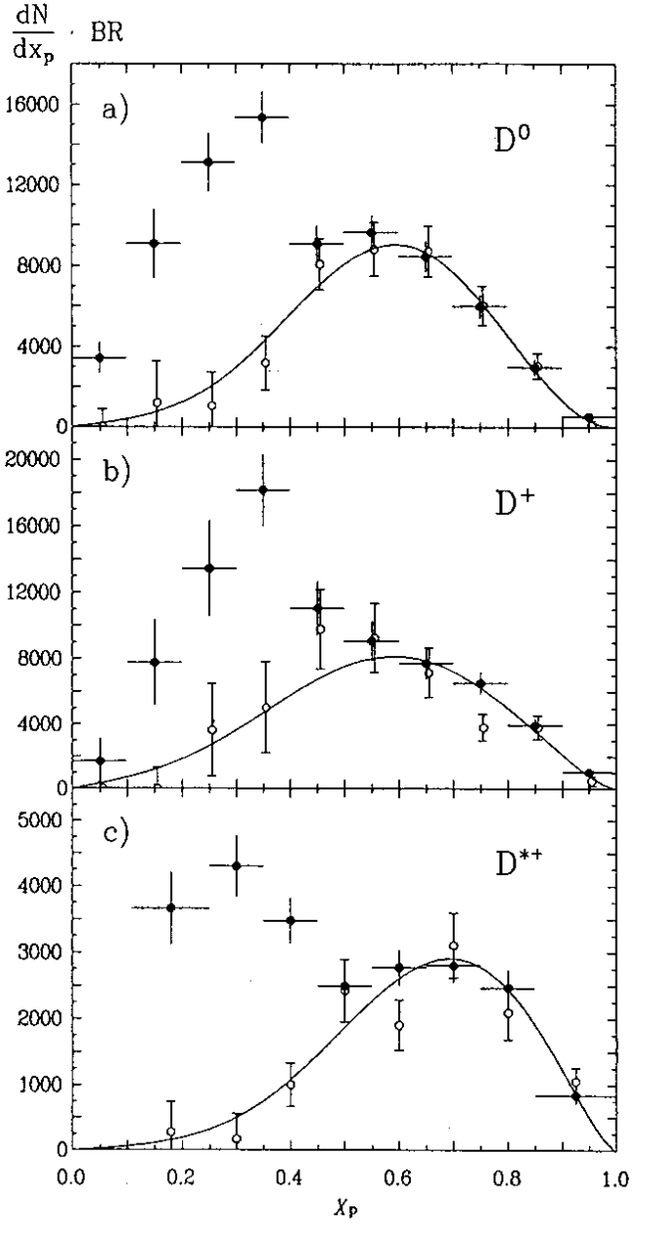

Figure 3

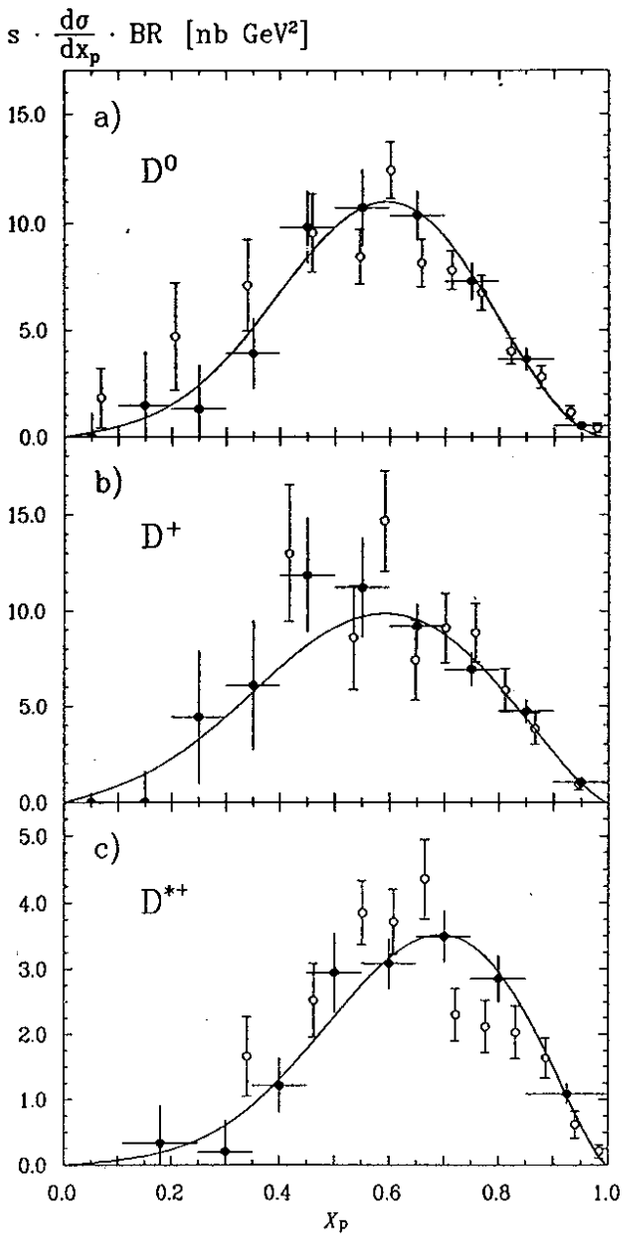

Figure 4

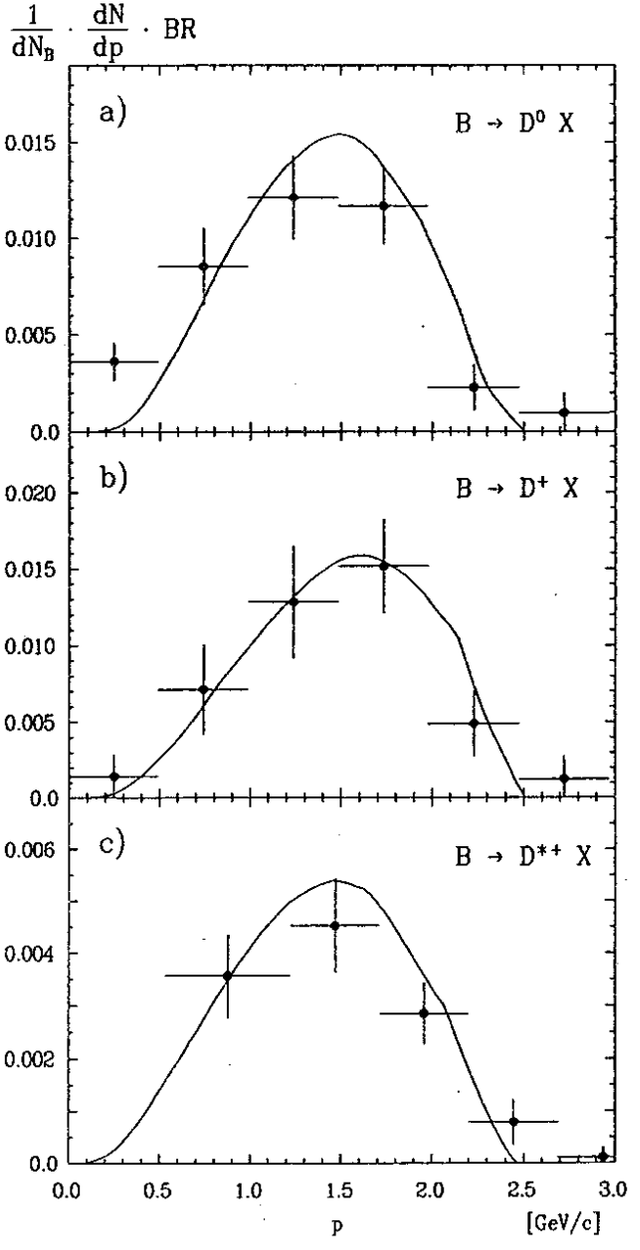

Figure 5